Published in final edited form as:
J Am Chem Soc. 1996 ; 118(49): 12261–12266. doi:10.1021/ja9623119.

Inductive Effects on the Energetics of Prolyl Peptide Bond Isomerization: Implications for Collagen Folding and Stability

Eric S. Eberhardt[†], **Nicholas Panisik Jr.**, and **Ronald T. Raines**[*]
Contribution from the Department of Biochemistry, University of Wisconsin–Madison, Madison, Wisconsin 53706-1569

Abstract

The hydroxylation of proline residues in collagen enhances the stability of the collagen triple helix. Previous X-ray diffraction analyses had demonstrated that the presence of an electron-withdrawing substituent on the pyrrolidine ring of proline residues has significant structural consequences [Panasik, N., Jr.; Eberhardt, E. S.; Edison, A. S.; Powell, D. R.; Raines, R. T. *Int. J. Pept. Protein Res.* **1994**, *44*, 262–269]. Here, NMR and FTIR spectroscopy were used to ascertain kinetic and thermodynamic properties of *N*-acetyl-[β,γ-^{13}C]D,L-proline methylester (**1**); *N*-acetyl-4(*R*)-hydroxy-L-proline [^{13}C]methylester (**2**); and *N*-acetyl-4(*R*)-fluoro-L-proline methylester (**3**). The pK_a's of the nitrogen atom in the parent amino acids decrease in the order: proline (10.8) > 4(*R*)-hydroxy-L-proline (9.68) > 4(*R*)-fluoro-L-proline (9.23). In water or dioxane, amide I vibrational modes decrease in the order: **1** > **2** > **3**. At 37 °C in dioxane, the rate constants for amide bond isomerization are greater for **3** than **1**. Each of these results is consistent with the traditional picture of amide resonance coupled with an inductive effect that results in a higher bond order in the amide C=O bond and a lower bond order in the amide C–N bond. Further, at 37 °C in water or dioxane equilibrium concentrations of the *trans* isomer increase in the order: **1** < **2** < **3**. Inductive effects may therefore have a significant impact on the folding and stability of collagen, which has a preponderance of hydroxyproline residues, all with peptide bonds in the *trans* conformation.

Introduction

Collagen is the principle structural protein in vertebrates.[1,2] *In vivo*, structural collagen consists of three polypeptide chains that form an extended right-handed triple helix.[3] Each polypeptide chain contains approximately three hundred repeats of the sequence: Gly–Xaa–Yaa, in which Xaa and Yaa are often L-proline (Pro) and 4(*R*)-hydroxy-L-proline (Hyp) residues, respectively. The hydroxylation of Pro residues is a post-translational modification catalyzed by the enzyme prolyl 4-hydroxylase. Defects in prolyl 4-hydroxylase activity have been associated with the aging process as well as a variety of diseases including arthritis and rheumatism.[4,5]

The biosynthesis of collagen has been studied extensively.[6–8] Collagen strands are synthesized as prepropeptides in which the pre sequence targets the polypeptide to the Golgi complex and there is removed by a protease. Three procollagen polypeptides then become covalently crosslinked through interstrand disulfide bonds within the pro region. The crosslinked chains are subjected to a variety of post-translational modifications before cleavage of the propeptide region and secretion into the extracellular matrix, where the chains fold into a triple helix. Of these modifications, the hydroxylation of proline residues

[†]Present address: Department of Chemistry, Bates College, Lewiston, ME 04240.

by prolyl 4-hydroxylase is the most prevalent, as Hyp constitutes approximately 10% of all collagen residues.

Numerous in vitro studies with procollagen and model peptides have explored the role of Hyp in the folding and stability of collagen.[5] Procollagen polypeptides that are deficient in Hyp can form triple helices, but these triple helices are unstable at room temperature.[9,10] Thermal denaturation studies have demonstrated that triple helix stability correlates with both overall Hyp content and Hyp position within the polypeptide.[11] Further, studies on model peptides suggest that peptide conformation is significantly affected by the hydroxylation of proline residues.[12,13]

Several models have been proposed in which Hyp mediates collagen stability by orienting water molecules to form interstrand hydrogen bonds.[14,15] In these models, no interstrand hydrogen bonds can be formed directly between the hydroxyl group of Hyp residues and any mainchain heteroatoms in the adjacent polypeptide chains of the triple helix.[16] Recently, a high-resolution X–ray diffraction analysis has revealed that water molecules do indeed form bridges between hydroxyl groups of Hyp residues and mainchain carbonyl groups.16 These bridges consist of 1, 2, or 3 water molecules.[17]

Because 25% of the residues in a typical collagen molecule are Pro or Hyp, the properties of these residues are likely to contribute greatly to collagen stability. In most peptide bonds, the *trans* (*Z*) isomer is greatly favored over the *cis* (*E*) isomer. In contrast, the *trans* isomer of a prolyl peptide bond is only slightly favored over the *cis* isomer. The interconversion of *cis* and *trans* isomers about prolyl peptide bonds has been identified as the rate-limiting step in protein folding pathways,[18] including that of collagen.[19–21] This attribute of collagen is not surprising because all peptide bonds in triple-helical collagen reside in the *trans* conformation. Moreover, the enzyme peptidyl–prolyl *cis–trans* isomerase (PPIase), which catalyzes the *cis–trans* interconversion of prolyl peptide bonds, accelerates the proper assembly of collagen molecules.[20]

The objective of this study is to determine the energetic consequences for the prolyl peptide bond of having an electron-withdrawing group in the 4(*R*) position of the pyrrolidine ring. Accordingly, we synthesized derivatives of proline having a hydroxyl or fluoro group at this position. We used these derivatives to determine the effect of electron withdrawal on (i) the pK_a of the prolyl nitrogen, (ii) the amide I vibrational mode of a prolyl peptide bond, and (iii) the kinetics and thermodynamics of prolyl peptide bond isomerization. The results have significance for understanding the folding and stability of collagen.

Results

Three proline derivatives were synthesized for this study: *N*-acetyl-[β,γ-^{13}C]D,L-proline methylester (**1**; Ac-Pro-OMe); *N*-acetyl-4(*R*)-hydroxy-L-proline [^{13}C]methylester (**2**; Ac-Hyp-OMe); and *N*-acetyl-4(*R*)-fluoro-L-proline methylester (**3**; Ac-Flp-OMe) (Chart 1).[22] The chirality of **2** is that found in natural collagen. The synthesis of **1**–**3** as the methylester avoids intramolecular hydrogen bonding, as had been observed in *N*-acetyl-L-proline[23] and *N*-acetyl-L-proline *N*-methylamide.[24,25] Compounds **1** and **2** were enriched with ^{13}C to improve the precision of data from ^{13}C NMR spectroscopy.[26,27] Compound **3** was synthesized because fluorine is more electronegative than is an oxygen and should therefore enhance any consequences of electron-withdrawal. Compound **3** was analyzed by ^{19}F NMR spectroscopy.[28]

Previously, we used X-ray diffraction analysis to determine the structure of unlabeled derivatives of **1**, **2**, and **3** (Table 1).[29] These structures indicated that the presence of electron-withdrawing substituents has significant structural consequences on the pyrrolidine

ring. First, the peptide bond is *cis* and the pyrrolidine ring has C^{γ} endo pucker in **1**; the peptide bond is *trans* and the pyrrolidine ring has C^{γ} exo pucker in **2** and **3**. Second, the nitrogen becomes increasingly pyramidalized as the electron-withdrawing ability of the substituent is stronger. This increase in pyramidalization is consistent with an increase in the sp^3 character of the prolyl nitrogen. Finally, although no difference was detected in bond lengths within the amide group, the C–C bonds adjacent to the electron-withdrawing substituent were shortened significantly.

Inductive Effect on pK_a

Changes in pK_a are consistent with an inductive effect. Such effects on the nitrogen of a proline ring are evident in the previously determined pK_a's of L-proline (10.64) and 4(*R*)-hydroxy-L-proline (9.66).[30] The lower pK_a of Hyp suggests that the hydroxyl group on the pyrrolidine ring is withdrawing electron density from the secondary amino group. Here, the pK_a's of the parent amino acids of **1**, **2**, and **3** were determined by monitoring the pH-dependencies of ^{1}H chemical shifts. The pK_a's of L-proline, 4(*R*)-hydroxy-L-proline, and 4(*R*)-fluoro-L-proline are 10.8, 9.68, and 9.23, respectively.[31] This trend is similar to that observed for ethylamine (10.63), ethanolamine (9.50), and 2-fluoroethylamine (8.79),[32] and is consistent with the manifestation of an inductive effect.

Inductive Effect on the Amide I Vibrational Mode

Changes in the frequency of vibrational modes can provide evidence for an inductive effect. The frequency of the amide I vibrational mode, which results primarily from the C=O stretching vibration, reports on the C=O bond order.33,34 In D_2O, the amide I vibrational modes of **1**, **2**, and **3** are maximal at 1608.10 cm^{-1}, 1613.08 cm^{-1}, and 1616.02 cm^{-1}, respectively (Figure 2). In dioxane, the amide I vibrational modes of **1**, **2**, and **3** are maximal at 1658.99 cm^{-1}, 1660.92 cm^{-1}, and 1664.78 cm^{-1}, respectively.[35] Thus in both solvents, the C=O bond order appears to increase in the order: **1** < **2** < **3**.[36] This apparent inductive effect on the amide I vibrational mode is similar to that observed in the C=O stretching frequency of 4-substituted camphors.[37]

Inductive Effect on k_{EZ} and k_{ZE}. The traditional picture of amide resonance predicts that an increase in C=O bond order is accompanied by a decrease in C–N bond order.38 Such a decrease in C–N bond order would facilitate *cis–trans* isomerization of the amide bond. In contrast, *ab initio* calculations suggest that little change in C=O bond order accompanies isomerization in the gas phase.[39–41] These calculations do not yet lead to a consensus about the C=O bond order when molecules of solvent are included.[42–45] We had observed that for peptides similar to **1**–**3** the barrier to isomerization ($\Delta G^{\ddagger}$) correlates with the frequency of the amide I vibrational mode (υ),[26,46] as predicted from the traditional view. To search for an inductive effect on the rate of *cis–trans* prolyl peptide bond isomerization (eq 1), we measured these rates for **1** and **3** in dioxane[47] and **1** and **2** in water[48] by using inversion transfer NMR spectroscopy.

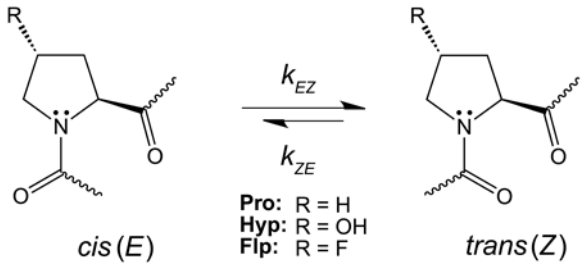

The effects of temperature on the *cis*-to-*trans* rate constant (k_{ZE}) and the *trans*-to-*cis* rate constant (k_{ZE}) are illustrated by Eyring plots in Figure 2. Values for $\Delta H^{\ddagger}$ and $\Delta S^{\ddagger}$ (±SE) were calculated from linear least-squares fits of the data in these plots to eq 2,[49]

$$\ln(k/T)=(-\Delta H^{\ddagger}/R)(1/T)+\Delta S^{\ddagger}/R+\ln(k_{B}/h) \quad (2)$$

where R is the gas constant, k_B is the Boltzman constant, and h is Planck's constant. The values of these activation parameters are listed in Table 2. Because k_{EZ} and k_{ZE} are lowered in protic solvents by the formation of hydrogen bonds to the oxygen of the prolyl peptide bond,[26,46,50] elevated temperatures were required to detect isomerization in water.

The free energy barriers to isomerization of **1**–**3** are almost exclusively enthalpic in origin. No significant difference was detected in the values of $\Delta H^{\ddagger}$ for **1** and **2**. A similar result had been obtained for Gly–Pro and Gly–Hyp in water.[51] The $\Delta H^{\ddagger}$ values do, however, differ for **1** and **3**. In considering proline derivatives **1** and **3** in dioxane, the enthalpic contribution to the barrier associated with k_{EZ} and k_{ZE} is reduced by 1.8 ± 1.1 and 3.6 ± 0.5 kcal/mol, respectively. If $\Delta H^{\ddagger}$ reflects the amount of bond breaking required for isomerization to occur, then these parameters suggest that the presence of fluorine on the pyrrolidine ring reduces the C–N bond order and hence the barrier to isomerization by withdrawing electron density towards the nitrogen.

Inductive Effect on $K_{Z/E}$

The corresponding *cis*-to-*trans* and *trans*-to-*cis* Eyring plots in Figure 2 are not parallel, indicating that the equilibrium constants are temperature dependent. The effects of temperature on the values of $K_{Z/E}$ (= k_{EZ}/k_{ZE}) were measured directly by NMR spectroscopy, and the resulting data are illustrated by van't Hoff plots in Figure 3. Values for $\Delta H°$ and $\Delta S°$ (±SE) were calculated from linear least-squares fits of the data in these plots to eq 3.

$$\ln K_{Z/E}=(-\Delta H^{\circ}/R)(1/T)+\Delta S^{\circ}/R \quad (3)$$

These values are listed in Table 3. This analysis assumes that the enthalpic and entropic differences between the *cis* and *trans* isomers are independent of temperature, that is, that $\Delta C_p° = 0$ for the reaction in eq 1.[52] The linear van't Hoff plots for the isomerization of **1**–**3** (Figure 3) and Ac-Gly-Pro-OMe[27] indicate that this assumption is likely to be valid for the reaction in eq 1.

In all conditions studied, the *trans* isomer of **1**–**3** is more stable than the *cis* isomer (Figure 3; Table 3). A similar result had been observed for Gly–Pro and Gly–Hyp in water at 25 °C.[51] Moreover, the values of $K_{Z/E}$ for **1**–**3** are dependent on temperature such that the *trans* isomer becomes increasingly favored as the temperature decreases. In other words, $\Delta H° < 0$ for the reaction in eq 1, as had been observed for Ac-Gly-Pro-OMe[27] and calculated with the 6-31G** basis set of the Gaussian 82 *ab initio* program.[53] In addition, the relative stability of the *trans* isomer is greater in water than dioxane. A similar solvent effect was observed for Ac-Gly-Pro-OMe.[27] Finally and perhaps most significantly, the values of $K_{Z/E}$ near room temperature increase in the order: **1** < **2** < **3**.

Discussion

The presence of electron-withdrawing substituents on the pyrrolidine ring can influence the structure of proline residues.[29] Here, such substituents are shown to affect the kinetics and thermodynamics of prolyl peptide bond isomerization.

Kinetics

Changes in the free energy of activation ($\Delta G^{\ddagger} = \Delta H^{\ddagger} - T\Delta S^{\ddagger}$) for prolyl peptide bond isomerization are proportional to changes in the frequency (n) of the amide I vibrational mode. In other words,

$$\Delta\Delta G^{\ddagger} = a_{\mathrm{I}}\Delta\upsilon \tag{4}$$

where a_{I} is an empirical parameter that varies from −0.022 to −0.030 kcal·cm/mol, depending on the peptide and type of solvent.[26,46] In all comparisons of **1**–**3**, $\Delta\upsilon < 8\ \mathrm{cm}^{-1}$ (Figure 2). This small frequency difference corresponds to $\Delta\Delta G^{\ddagger} < 0.23$ kcal/mol or only a <1.5-fold change in rate constant at 37 °C. For **1** and **3**, this small difference is apparent in $\Delta H^{\ddagger}$, and in k_{EZ} and k_{ZE} calculated by extrapolation of the Eyring plots to 37 °C (Table 2), which is the approximate physiological temperature of vertebrates. For **1** and **2**, these subtle differences are not detectable by our kinetic assay. Still, X-ray diffraction analyses (Table 1), pK_{a} determinations, and amide I vibrational modes (Figure 2) suggest that **2**, like **3**, has more electron density residing on the nitrogen of the prolyl peptide bond than does **1**.

A typical collagen molecule has approximately thirty Hyp residues. The folding of the collagen triple helix is therefore likely to be accelerated by the cumulative effect of electron-withdrawing hydroxyl groups attached to C$^{\gamma}$ of the pyrrolidine rings. Moreover, our results predict that the incorporation of 4(*R*)-fluoroproline into collagen or other proteins in which folding is limited by prolyl peptide bond isomerization would lead to a measurable increase in folding rate.

Thermodynamics

The value of $K_{Z/E}$ for a prolyl peptide bond is mediated by contacts between C$^{\alpha}$ of the adjacent residue and C$^{\alpha}$ or C$^{\delta}$ of the proline residue.[18] The value of $K_{Z/E}$ for **1**–**3** increases as the electron-withdrawing ability of the C$^{\delta}$ substituent increases. The origin for this increase may be the shorter C$^{\gamma}$–C$^{\delta}$ bond. The C$^{\gamma}$–C$^{\delta}$ bond length is decreased by (0.013 ± 0.004) Å in **2** and (0.016 ± 0.003) Å in **3**.[29] In effect, the hydroxyl group or fluorine atom attached to C$^{\gamma}$ serves to pull C$^{\delta}$ away from C$^{\alpha}$ of the adjacent residue. This structural manifestation of the inductive effect should increase the stability of the *trans* isomer, thereby increasing $K_{Z/E}$.

An alternative explanation for the observed increase in $K_{Z/E}$ is based on stereoelectronics and its effect on pyrrolidine ring pucker. Electron-withdrawing groups on C$^{\gamma}$ can in theory alter the preferred conformation of the pyrrolidine ring. Specifically, the tendency of molecules to adopt the conformation that has the maximum number of gauche interactions between adjacent polar bonds has been termed the “gauche effect”.[54] The gauche effect has been invoked to explain the conformational preferences of double-helical nucleic acids,[55,56] but not that of Hyp residues. A gauche effect based on the nitrogen and the hydroxyl group of **2** or fluorine of **3** would impose C$^{\gamma}$-exo pucker on the pyrrolidine rings of **2** and **3**. This pucker was indeed observed in crystalline **2** and **3** (but not **1**; Table 1),[29] and in all of the Hyp residues (but only half of the Pro residues) in crystalline collagen.[16] The role of the

gauche effect in collagen structure and stability is the object of on-going work in our laboratory.

In water at 37 °C, $K_{Z/E}$ is 1.5-fold larger for **2** than **1** (Table 3). Because triple-helical collagen typically contains approximately 3 × 30 Hyp residues, the effect of stabilizing the *trans* isomer of each Hyp residue therefore has a cumulative effect on collagen stability. This analysis does not exclude a role for water in stabilizing the collagen triple helix.[17] It does, however, suggest that the inductive effect can contribute to this stability.

Conclusions

An electron-withdrawing substituent at the 4(*R*) position of a pyrrolidine ring has significant structural and energetic consequences. An apparent inductive effect increases pyramidalization of the prolyl nitrogen, lowers the nitrogen pK_a, shifts the amide I vibrational mode downfield, and reduces the energetic barrier to isomerization. Furthermore, such a substituent alters the prolyl peptide bond equilibrium constant. These effects have important implications for collagen folding and stability of triple-helical collagen, in which all peptide bonds are in the *trans* conformation.

Experimental Section

Materials

tert-Butoxycarbonyl-[β,γ-^{13}C]-D,L-proline methylester,[22] *N*-acetyl-4(*R*)-acetoxy-L-proline methylester,[29] and **3**[29] were synthesized as described previously. L-Proline, 4(*R*)-hydroxyl-L-proline, and all other reagents were from Aldrich Chemical (Milwaukee, WI) and were used without further purification unless indicated otherwise. Solvents for NMR spectroscopy in pre-packaged ampules were from Aldrich Chemical and were used without further purification.

N-Acetyl-[β,γ-^{13}C]-D,L-Proline Methylester (1)

tert-Butoxycarbonyl-[β,γ-^{13}C]-D,L-proline methylester (0.50 g, 2.2 mmol) was added to a solution (10 mL) of dioxane containing HCl (4 N). The resulting solution was stirred at 25 °C for 30 min, then concentrated, dried, and stirred with acetic anhydride (25 mL) at 25 °C for 16 h. The reaction mixture was concentrated under reduced pressure, and the concentrate was dissolved in ethyl acetate. The resulting solution was washed with 1 N HCl (3 × 50 mL), 1 N NaOH (3 × 50 mL), and saturated aqueous NaCl. The organic extract was dried over $MgSO_4$, filtered, and concentrated to a yellow oil. The crude product was loaded on to a 10 g silica column in $CHCl_3$ and eluted with a gradient of methanol (1–5% v/v) in $CHCl_3$ to yield **1** as a white solid (0.37 g, 85%). R_f (ethylacetate) = 0.17. MH^+(FAB) = 173.10. ^{1}H NMR (400 MHz, $CDCl_3$) δ 4.55 (d br, 1H, $C_1{}^{\alpha}H$; minor isomer at 4.46), 3.76 (m, 1H, $C_1{}^{\delta}H$; minor isomer at 3.61), 3.62 (s, 3H, C_2H_3; minor isomer at 3.69), 3.47 (m, 1H, $C_1{}^{\delta}H'$; minor isomer at 3.33), 2.28 (m, 1H, $C_1{}^{\beta}H$; minor isomer at 2.09), 2.03 (s, 3H, C_0H_3; minor isomer at 1.95) 2.01 (m, 2H, $C_1{}^{\gamma}H$; minor isomer at 1.82), 1.98 (m, 1H, $C_1{}^{\beta}H'$; minor isomer at 1.83). ^{13}C NMR ($CDCl_3$) δ 47.52 ($^{\delta}C_1$; minor isomer 46.04), 29.19 ($^{\beta}C_1$; minor isomer 31.23).

N-Acetyl-4(*R*)-Hydroxy-L-Proline [^{13}C]Methylester (2)

Anhydrous potassium carbonate (0.01g, 0.08 mmol) was added to a solution of *N*-acetyl-4(*R*)-acetoxy-L-proline methylester (0.15 g, 0.66 mmol) in 5 g of methanol enriched to 99.98% with ^{13}C. The resulting slurry was stirred at 25 °C for 30 min. The mixture was filtered, and the filtrate was concentrated under reduced pressure. The crude product was loaded on to a 10 g silica column and eluted with ethyl acetate:hexanes (1:2 v/v) to yield **2** as a clear oil (0.079 g, 64%). R_f (ethyl acetate) = 0.17. MH^+(FAB) = 189.14. ^{1}H NMR

($CDCl_3$) δ 4.62 (s, 1H, $C_1^{\gamma}H$; minor isomer at 4.49), 4.33 (t, 1H; $C_1^{\alpha}H$; minor isomer at 4.25), 3.80 (s, 1H, $C_1^{\delta 2}H$), 3.55 (s, 3H, OCH_3; minor isomer at 3.70), 3.35 (d, 1H, $C_1^{\delta 2}H$; minor isomer at 3.42), 2.91 (s, broad, 1H, OH), 2.12 (m, $C_1^{\beta}H$; minor isomer at 2.26), 1.90 (s, 3H, $COCH_3$; minor isomer at 1.78), 1.86 (m, 1H, $C_1^{\beta}H$); ^{13}C NMR ($CDCl_3$) δ 58.40 (C_2; minor isomer at 57.24).

NMR Spectroscopy

Values of pK_a, k_{EZ}, k_{ZE}, and $K_{Z/E}$ were determined by NMR spectroscopy.

pK_a Determinations

The secondary amine pK_a's of the parent amino acids of **1**, **2**, and **3** were determined by pH-titration monitored by ^1H NMR spectroscopy. Experiments were performed on a Bruker AM500 instrument (498.68 MHz) using a 5 mm ^1H probe and ^1H bandpass filter. Solvent suppression was applied to the water signal, and a deuterium oxide insert was used to provide an external lock. Stock solutions (0.40 M; 50 mL) of L-proline, 4(*R*)-hydroxy-L-proline, and 4(*R*)-fluoro-L-proline (which was prepared by hydrolysis of *tert*-butoxycarbonyl-4(*R*)-fluoro-L-proline methylester) were prepared in 0.10 M sodium phosphate buffer, pH 7.0. An aliquot (0.40 mL) was removed from the stock solution, and the chemical shift difference ($\Delta\delta$) between the α and β protons [for L-proline and 4(*R*)-hydroxy-L-proline], or the α and δ protons [for 4(*R*)-fluoro-L-proline], were measured at 25 °C. The aliquot was returned to the stock solution, and the pH of that solution was decreased by approximately 0.1 units by the addition of an aliquot (0.10 mL) of 1 N KOH. Values of pK_a were determined by nonlinear least-squares fits of the $\Delta\delta$ and pH data to the Henderson–Hasselbalch equation.

Kinetics

The *cis–trans* isomerization rate of **1**–**3** were determined by ^{13}C (for **1** and **2**) or ^{19}F (for **3**) NMR inversion transfer NMR spectroscopy.[57–59] Experiments were performed on a Bruker AM500 instrument (^{13}C 125.68 MHz) using a 5 mm broadband probe, ^1H bandpass filter, and ^{13}C lowpass filter; or a Bruker AM400 instrument (^{19}F 376.48 MHz) using a 5 mm ^{19}F probe, ^1H bandpass filter, ^{19}F bandstop, and ^{19}F bandpass filter.

Samples of **1**, **2**, and **3** were prepared at concentrations of 0.10 M and 1.0 mM in dioxane-d_8. Aqueous samples contained 20% (v/v) ^2H_2O in 0.10 M sodium phosphate buffer, pH 7.2. The rate of prolyl peptide bond isomerization cannot be detected by this method at room temperature. Experiments were therefore conducted at elevated temperatures, 310–360 K. Temperature settings of the spectrometer were calibrated to within 1 °C by reference to a glycol standard.

Spectra were obtained using the inversion transfer pulse sequence in eq 5.

$$90^{\circ}_x - \frac{1}{2}\Delta\delta - 90^{\circ}_x - \tau - 90^{\circ}_x \quad (5)$$

Briefly, the signal for one isomer is placed on a carrier frequency, and the intensity change of the signal for the other isomer is monitored during its recovery from a selective 180° pulse. The time-dependence of the change in signal intensity allows for the determination of the isomerization rate.

The time-dependent peak height [$M(\tau)$] for each resonance was fit by nonlinear least-squares to eq 6 and 7[57] with SIGMA PLOT 4.16 (Jandel Scientific; San Rafael, CA).

$$M_a(\tau)=C_{1e}{}^{\lambda_1\tau}+C_{2e}{}^{\lambda_2\tau}+M_a^{\infty} \quad (6)$$

$$M_b(\tau)=C_{3e}{}^{\lambda_1\tau}+C_{4e}{}^{\lambda_2\tau}+M_b^{\infty} \quad (7)$$

In eq 6 and 7, the "a" subscript refers to the *cis* resonance, the "b" subscript refers to the *trans* resonance, and M^{∞} refers to the peak height at equilibrium. At each temperature, complementary experiments were performed in which the *cis* or *trans* peak was placed on the carrier frequency. Data from both experiments were fit to eq 6 and 7, with the *cis* constants denoted as in eq 5 and 6 and the *trans* constants denoted as C_1*, C_2*, C_3*, C_4*, λ_{1a}, and λ_{2a}. Values of k_{ia} and k_{ib} were then calculated by using eq 8 and 9.[57]

$$k_{ia}=\frac{(C_1^*\lambda_{1a}+C_2^*\lambda_{2a})(C_3+C_4)-(C_3^*+C_4^*)(C_1\lambda_1+C_2\lambda_2)}{(C_3^*+C_4^*)(C_1+C_2)-(C_1^*+C_2^*)(C_3+C_4)} \quad (8)$$

$$k_{ib}=\frac{(C_3^*\lambda_{1a}+C_4^*\lambda_{2a})(C_1+C_2)-(C_3\lambda_1+C_4\lambda_2)(C_1^*+C_2^*)}{(C_3+C_4)(C_1^*+C_2^*)-(C_3^*+C_4^*)(C_1+C_2)} \quad (9)$$

The isomerization rate constants, k_{EZ} and k_{ZE}, were calculated by using eq 10 and 11, where α is the ratio of the *cis* line width to the *trans* line width.

$$k_{EZ}=\frac{(C_3\lambda_1+C_4\lambda_2)+k_{ib}(C_3+C_4)}{\alpha(C_1+C_2)} \quad (10)$$

$$k_{ZE}=\frac{\alpha(C_1\lambda_1+C_2\lambda_2)+k_{ia}(C_1+C_2)}{C_3+C_4} \quad (11)$$

Thermodynamics

The equilibrium constants for the interconversion of the *cis* and *trans* isomers of **1**–**3** were determined by measuring the peak areas of the ^{13}C (for **1** and **2**) or ^{19}F (for **3**) resonances for the two isomers. Peak areas were measured with the program FELIX 2.3 (Technologics; San Diego, CA). Experiments were conducted at 300–355 K. Equilibrium constants ($K_{Z/E}$ = *trans*/*cis*) were calculated directly from the peak areas.

FTIR Spectroscopy

FTIR spectra were recorded on a Nicolet 5PC spectrometer. Experiments were performed at 25 °C using NaCl or CaF_2 plates, or a ZnSe crystal in a Spectra Tech circle cell. The frequency of amide I vibrational modes was determined to within 2 cm^{-1}.

Samples of **1**, **2**, and **3** were prepared at concentrations of 0.10 M and 1.0 mM in dioxane (which had been distilled from CaH_2) and in D_2O. No concentration effects were observed for **1** and **3** in either solvent. A second vibrational mode was present in the amide I region in

a 0.10 M solution of **2**. This mode was absent in a 1.0 mM solution of **2**. Thus, all FTIR spectra in dioxane were recorded on 1.0 mM solutions of **1**–**3**.

Acknowledgments

This work was supported by grant AR44276 (NIH). NMR experiments were performed at the National Magnetic Resonance Facility at Madison (NMRFAM), which is supported by grant RR02301 (NIH).

Notes and References

1. Ramachandran, GN.; Reddi, AH., editors. Biochemistry of Collagen. Plenum Press; New York: 1976.
2. Nimni, ME. Collagen. CRC Press; Boca Raton, Fl: 1988.
3. Rich A, Crick FHC. J Mol Biol. 1961; 3:483–506. [PubMed: 14491907]
4. Baldwin CT, Constanteu CD, Dumars KW, Prockop DJ. J Biol Chem. 1989; 264:3002–3006. [PubMed: 2914942]
5. Kadler, K. Protein Profile. 1994. p. 519-638.
6. Prockop DJ, Kivirikko KI, Tuderman L, Guzman NA. N Eng J Med. 1979; 301:13–23.
7. Prockop DJ. New Engl J Med. 1992; 326:540–546. [PubMed: 1732793]
8. Brodsky B, Shah NK. FASEB J. 1995; 9:1537–1546. [PubMed: 8529832]
9. Berg RA, Prockop DJ. Biochem Biophys Res Comm. 1973; 52:115–120. [PubMed: 4712181]
10. Rao NV, Adams E. Biochem Biophys Res Comm. 1979; 86:654–660. [PubMed: 426812]
11. Sakakibara S, Inouye K, Shudo K, Kishida Y, Kobayashi Y, Prockop DJ. Biochem Biophys Acta. 1973; 303:198–202. [PubMed: 4702003]
12. Bruckner P, Bächinger HP, Timpl R, Engel J. Eur J Biochem. 1978; 90:593–603.
13. Chopra RK, Ananthanarayanan VS. Proc Natl Acad Sci USA. 1982; 79:7180–7184. [PubMed: 6296823]
14. Ramachandran GN, Bansal M, Bhatnagar RS. Biochim Biophys Acta. 1973; 322:166–171. [PubMed: 4744330]
15. Suzuki E, Fraser RDB, MacRae TP. Int J Biol Macromol. 1980; 2:54–56.
16. Bella J, Eaton M, Brodsky B, Berman HM. Science. 1994; 266:75–81. [PubMed: 7695699]
17. Bella J, Brodsky B, Berman HM. Structure. 1995; 3:893–906. [PubMed: 8535783]
18. Brandts JF, Halvorson HR, Brennan M. Biochemistry. 1975; 14:4853–4963.
19. Bächinger HP, Bruckner P, Timpl R, Prockop DJ, Engel J. Eur J Biochem. 1980; 106:619–632. [PubMed: 7398630]
20. Bächinger HP. J Biol Chem. 1987; 262:17144–17148. [PubMed: 3316229]
21. Liu X, Siegel DL, Fan P, Brodsky B, Baum J. Biochemistry. 1996; 35:4306–4313. [PubMed: 8605179]
22. Hinck AP, Eberhardt ES, Markley JL. Biochemistry. 1993; 32:11810–11818. [PubMed: 8218252]
23. Detar DF, Luthra NP. J Am Chem Soc. 1977; 99:1232–1244. [PubMed: 833398]
24. Matsuzaki T, Iitaka Y. Acta Crystallogr. 1971; B27:507–516.
25. Liang GB, Rito CJ, Gellman SH. Biopolymers. 1992; 32:293–301. [PubMed: 1581548]
26. Eberhardt ES, Loh SN, Hinck AP, Raines RT. J Am Chem Soc. 1992; 114:5437–5439.
27. Eberhardt ES, Loh SN, Raines RT. Tetrahedron Lett. 1993; 34:3055–3056. [PubMed: 20628473]
28. London RE, Davis DG, Vavrek RJ, Stewart JM, Handschumacher RE. Biochemistry. 1990; 29:10298–10302. [PubMed: 2261473]
29. Panasik N Jr, Eberhardt ES, Edison AS, Powell DR, Raines RT. Int J Pept Protein Res. 1994; 44:262–269. N.B.: The stereochemistry at the 4 position of **2** and **3** was reported incorrectly in the text of ref 29. [PubMed: 7822103]
30. Fasman, GD., editor. Practical Handbook of Biochemistry and Molecular Biology. CRC Press; Boca Raton, FL: 1989.
31. The error in these values is ±0.10, which is the error in measuring pH.

32. Hall HKJ. J Am Chem Soc. 1957; 79:5441.
33. Krimm, S.; Bandekar, J. Advances in Protein Chemistry. Vol. 38. Academic Press; New York: 1986. p. 183-364.
34. Jackson M, Mantsch HH. Crit Rev Biochem Molec Biol. 1995; 30:95–120. [PubMed: 7656562]
35. The solvent effect of approximately 50 cm^{-1} is consistent with those observed for other amides. For references, see: Reichardt, C. Solvents and Solvent Effects in Organic Chemistry. VCH; New York: 1988. p. 313-319.
36. A second vibrational mode was present in the amide I region of a 0.10 M solution of **2**. This low frequency mode was absent in a 1.0 mM solution of **2**. This second vibrational mode was likely the result of a hydrogen bond from the hydroxyl group of one molecule of **2** to the amide carbonyl group of another molecule of **2**, as was observed in crystalline **2** (ref. [29]). To minimize this apparent aggregation, FTIR experiments in dioxane were performed on 1.0 mM solutions of **1–3**.
37. Laurence C, Berthelot M, Lucon M, Helbert M, Morris DG, Gal J-F. J Chem Soc Perkin Trans. 1984; II:705–710.
38. Pauling, L. The Nature of the Chemical Bond. 3. Cornell University Press; Ithaca, NY: 1960. p. 281-282.
39. Wiberg KB, Laidig KE. J Am Chem Soc. 1987; 109:5935–5943.
40. Laidig KE, Bader RFW. J Am Chem Soc. 1991; 113:6312–6313.
41. Wiberg KB, Breneman CM. J Am Chem Soc. 1992; 114:831–840.
42. Mirkin NG, Krimm S. J Am Chem Soc. 1991; 113:9742–9747.
43. Duffy EM, Severance DL, Jorgensen WL. J Am Chem Soc. 1992; 114:7535–7542.
44. Luque FJ, Orozco M. J Org Chem. 1993; 58:6397–6405.
45. Wiberg KB, Rablen PR, Rush DJ, Keith TA. J Am Chem Soc. 1995; 117:4261–4270.
46. Eberhardt ES, Raines RT. J Am Chem Soc. 1994; 116:2149–2150.
47. A kinetic analysis of **2** in dioxane was precluded by aggregation. Decreasing the concentration of **2** from 0.10 M to 1.0 mM resulted in a 10–20% increase in isomerization rates and an increase in error from <10% to >60%, depending on the temperature. The aggregation of **2** in dioxane during NMR spectroscopy experiments was also observed by FTIR spectroscopy (ref. [36]).
48. Compound **3** could not be analyzed by ^{19}F NMR spectroscopy in water because of overlap of the two ^{19}F resonances at most temperatures.
49. Eyring H. J Chem Phys. 1935; 3:107–115.
50. Radzicka A, Acheson SA, Wolfenden R. Bioorg Chem. 1992; 20:382–386.
51. Mariappan SVS, Rabenstein DL. J Org Chem. 1992; 57:6675–6678.
52. Stauffer DA, Barrans RE Jr, Dougherty DA. J Org Chem. 1990; 55:2762–2767.
53. Radzicka A, Pedersen L, Wolfenden R. Biochemistry. 1988; 27:4538–4541. [PubMed: 3166998]
54. Brunck TK, Weinhold F. J Am Chem Soc. 1979; 101:1700–1709.
55. Guschlbauer W, Jankowski K. Nucleic Acids Res. 1980; 8:1421–1433. [PubMed: 7433125]
56. Plavec J, Thibaudeau C, Chattopadhyaya J. J Am Chem Soc. 1994; 116:6558–6560.
57. Forsén S, Hoffman RA. J Chem Phys. 1963; 39:2892–2901.
58. Grathwohl C, Wüthrich K. Biopolymers. 1981; 20:2623–2633.
59. Led JJ, Gesmar H. J Mag Res. 1982; 49:444–463.

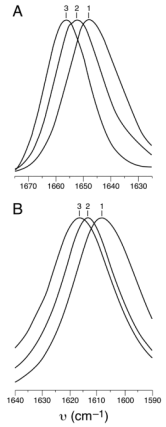

Figure 1.

(a) Amide I vibrational modes of **1** (υ_{max} = 1658.99 cm^{-1}), **2** (1660.92 cm^{-1}), and **3** (1664.78 cm^{-1}) in dioxane. (b) Amide I vibrational mode of **1** (υ_{max} = 1608.10 cm^{-1}), **2** (1613.08 cm^{-1}), and **3** (1616.02 cm^{-1}) in D_2O.

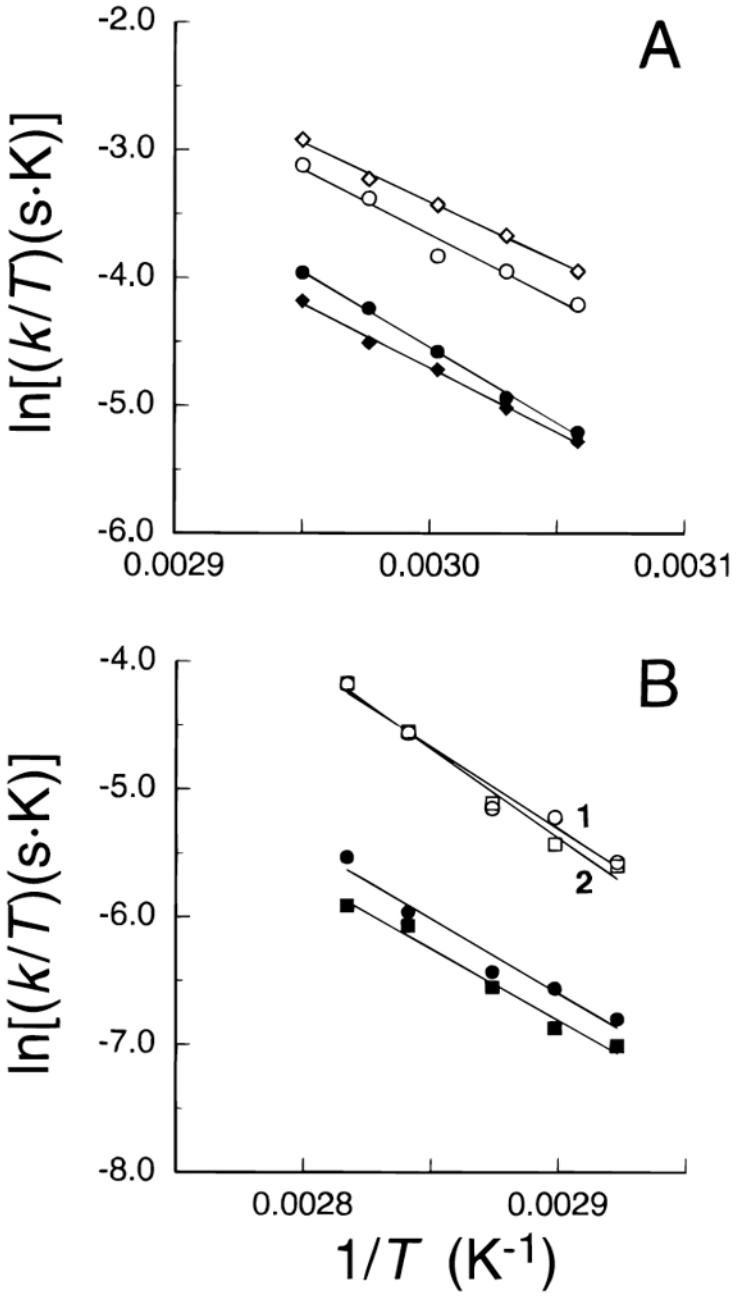

Figure 2.

(a) Eyring plots of the *cis*-to-*trans* isomerization of **1** (○) and **3** (◇), and the *trans*-to-*cis* isomerization of **1** (●) and **3** (◆) in dioxane. (b) Eyring plots of the *cis*-to-*trans* isomerization of **1** (○) and **2** (□), and the *trans*-to-*cis* isomerization of **1** (●) and **2** (■) in 0.10 M sodium phosphate buffer, pH 7.2.

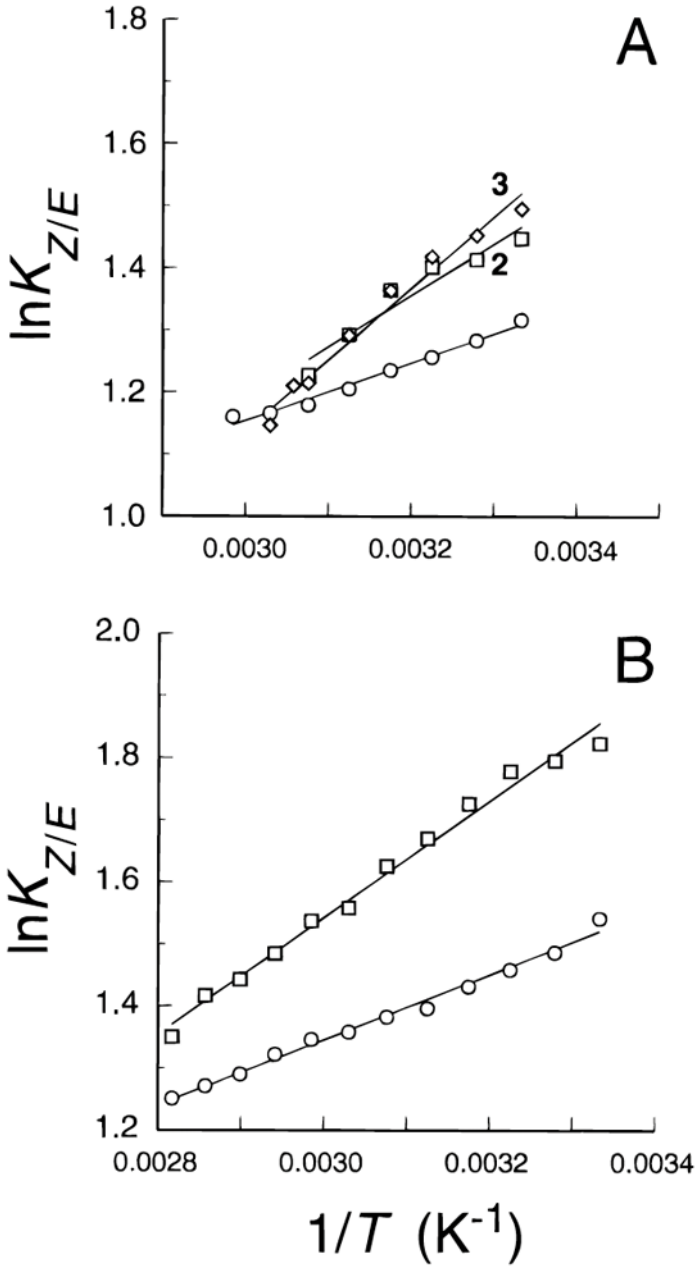

Figure 3.
(a) Van't Hoff plots of the *cis*-to-*trans* isomerization of **1** (○), **2** (□), and **3** (◇) in dioxane. (b) Van't Hoff plots of the *cis*-to-*trans* isomerization of **1** (○) and **2** (□) in 0.10 M sodium phosphate buffer, pH 7.2.

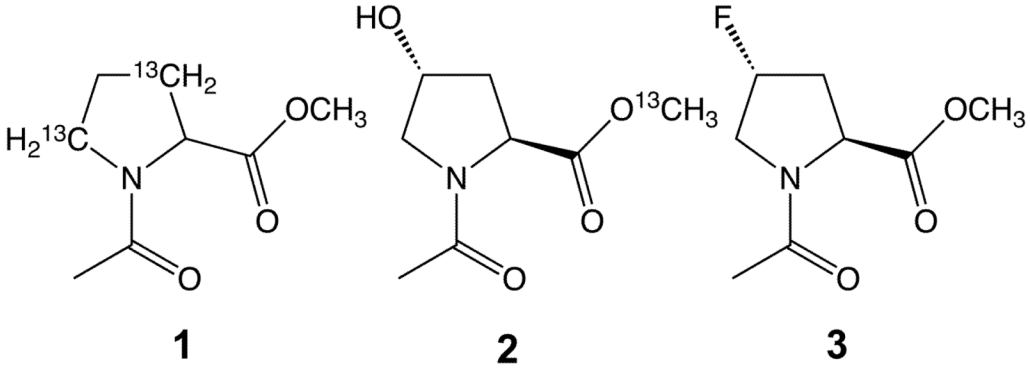

Chart 1.

Table 1

Summary of X-Ray Diffraction Analyses [a]

compound[b]	pyrrolidine ring pucker	peptide bond isomer	pyramidalization (δ;deg)[c]
1	C^{γ}-endo	*cis*	1.05
2a	C^{γ}-exo	*trans*	−9.24
2b	C^{γ}-exo	*trans*	−1.52
3a	C^{γ}-exo	*trans*	−16.31
3b	C^{γ}-exo	*trans*	−3.54

[a] From ref. 29.

[b] The unit cells of crystalline **2** and **3** contain two molecules. In crystalline **2**, the hydroxyl group of molecule **2a** donates a hydrogen bond to the amide oxygen of molecule **2b**.

[c] The parameter δ refers to the angle that the amide C–N bond makes with the plane defined by N, C^{α}, and C^{δ} of the pyrrolidine ring.

Table 2

Activation Parameters for Isomerization of **1**–**3**

compound	solvent	process	$\Delta H^{\ddagger a}$ (kcal/mol)	$\Delta S^{\ddagger a}$ [cal/(mol·K)]	k (37 °C) ^{b} (s^{-1})
1	dioxane	*cis-to-trans*	20.2 ± 1.0	6.2 ± 0.4	0.86 ± 0.44
		trans-to-cis	23.5 ± 0.3	14.4 ± 1.0	0.25 ± 0.05
	water	*cis-to-trans*	25.5 ± 1.4	16.2 ± 1.1	0.024 ± 0.17
		trans-to-cis	23.2 ± 1.3	7.1 ± 3.4	0.010 ± 0.008
2	dioxane	*cis-to-trans*		(not determined[47])	
		trans-to-cis		(not determined[47])	
	water	*cis-to-trans*	27.7 ± 1.2	22.5 ± 1.2	0.016 ± 0.10
		trans-to-cis	22.2 ± 0.8	3.8 ± 0.2	0.010 ± 0.004
3	dioxane	*cis-to-trans*	18.4 ± 0.4	1.2 ± 0.1	1.3 ± 0.3
		trans-to-cis	19.9 ± 0.4	3.2 ± 0.1	0.31 ± 0.06
	water	*cis-to-trans*		(not determined[48])	
		trans-to-cis		(not determined[48])	

[a] Values ± SE were obtained by linear least-squares fitting of the data in Figure 2 to eq 2.

[b] Values ± SE were calculated with eq 2.

Table 3

Thermodynamic Parameters for Isomerization of **1**–**3**

compound	solvent	$\Delta H°$ [a] (kcal/mol)	$\Delta S°$ [a] [cal/(mol·K)]	$K_{Z/E}$ (37 °C)[b]
1	dioxane	−1.04 ± 0.01	−0.84 ± 0.04	3.5 ± 0.1
	water	−1.04 ± 0.02	−0.46 ± 0.05	4.3 ± 0.2
2	dioxane	−1.65 ± 0.12	−2.58 ± 0.38	4.0 ± 1.1
	water	−1.87 ± 0.03	−2.55 ± 0.03	5.8 ± 0.3
3	dioxane	−2.29 ± 0.07	−4.60 ± 0.23	4.1 ± 0.7
	water	(not determined[48])		6.2 ± 0.1 [c]

[a] Values ± SE were obtained by linear least-squares fitting the data in Figure 3 to eq 3.

[b] Values ± SE were calculated with eq 3.

[c] Measured directly.